Cerebral Cortex September 2011;21:2065–2074
doi:10.1093/cercor/bhq281
Advance Access publication January 31, 2011

Nitric Oxide Signaling Modulates Synaptic Transmission during Early Postnatal Development

Csaba Cserép[1], András Szőnyi[1], Judit M. Veres[2], Beáta Németh[2], Eszter Szabadits[1], Jan de Vente[3], Norbert Hájos[2], Tamás F. Freund[1] and Gábor Nyiri[1]

[1]Laboratory of Cerebral Cortex Research and [2]Laboratory of Network Neurophysiology, Department of Cellular and Network Neurobiology, Institute of Experimental Medicine, Hungarian Academy of Sciences, H-1083 Budapest, Hungary and [3]European Graduate School of Neuroscience, Department of Psychiatry and Neuropsychology, Division of Cellular Neuroscience, Maastricht University, 6200 MD Maastricht, The Netherlands

Address correspondence to Gábor Nyiri, Institute of Experimental Medicine, Hungarian Academy of Sciences, Szigony u. 43, H-1083 Budapest, Hungary. Email: nyiri@koki.hu.

Early γ-aminobutyric acid mediated (GABAergic) synaptic transmission and correlated neuronal activity are fundamental to network formation; however, their regulation during early postnatal development is poorly understood. Nitric oxide (NO) is an important retrograde messenger at glutamatergic synapses, and it was recently shown to play an important role also at GABAergic synapses in the adult brain. The subcellular localization and network effect of this signaling pathway during early development are so far unexplored, but its disruption at this early age is known to lead to profound morphological and functional alterations. Here, we provide functional evidence—using whole-cell recording—that NO signaling modulates not only glutamatergic but also GABAergic synaptic transmission in the mouse hippocampus during the early postnatal period. We identified the precise subcellular localization of key elements of the underlying molecular cascade using immunohistochemistry at the light—and electron microscopic levels. As predicted by these morpho-functional data, multineuron calcium imaging in acute slices revealed that this NO-signaling machinery is involved also in the control of synchronous network activity patterns. We suggest that the retrograde NO-signaling system is ideally suited to fulfill a general presynaptic regulatory role and may effectively fine-tune network activity during early postnatal development, while GABAergic transmission is still depolarizing.

Keywords: GABAergic synapse, hippocampus, nNOS, retrograde signaling, synchronous activity

Introduction

Recruitment of γ-aminobutyric acid mediated (GABAergic) inhibition shapes synchronous population events in the adult brain. However, during the early postnatal period, GABAergic synaptic transmission exerts a complex depolarizing (excitatory/shunting inhibitory) effect, which is shifted to hyperpolarizing (inhibitory) only during the second postnatal week (Ben-Ari et al. 2007). Hence, the role of GABA signaling during the early postnatal period is associated with the generation of the first synapse-driven synchronous network activity patterns—giant depolarizing potentials in vitro (Ben-Ari et al. 2007; Crepel et al. 2007) or synchronous burst activity in vivo (Sipila et al. 2006). GABAergic synaptic transmission and synchronous activity of cell assemblies are fundamental to the formation of functional networks (Ge et al. 2006; Mohajerani and Cherubini 2006; Akerman and Cline 2007; Cancedda et al. 2007; Wang and Kriegstein 2008). However, the regulation of these events is poorly understood.

The blockade of nitric oxide (NO) signaling during development leads to disturbances in dendrite morphology and to a reduction in synapse numbers (Sánchez-Islas and León-Olea 2004; Morales-Medina et al. 2007). These data reflect the developmental importance of the NO pathway and raise the question whether it manifests at the synaptic or networks levels or both and whether GABAergic transmission that normally shapes network patterns is also under the control of retrograde NO signaling during early postnatal development.

NO is an effective modulator of synaptic transmission in the adult hippocampus (Burette et al. 2002; Bon and Garthwaite 2003; Makara et al. 2007; Szabadits et al. 2007). The NO-sensitive guanylyl cyclase (NOsGC) that contains an α and a β subunit, is the NO receptor in the brain (Koesling et al. 2004), and the only cGMP-producing enzyme in hippocampal neurons (Teunissen et al. 2001). Accordingly, NO induces the production of the second messenger cGMP, which may alter the probability of vesicular release depending on the type of terminal and brain region (Garthwaite 2008).

In low-resolution immunocytochemical and in situ hybridization studies, the rodent hippocampus was found to express neuronal nitric oxide synthase (nNOS) and NOsGC already during the early postnatal days (Giuili et al. 1994; Chung et al. 2004). However, the cellular and subcellular localization of the elements of this signaling pathway and their effects on synaptic transmission and network activity during development remained unexplored.

Here, we showed that nNOS was present in pyramidal cells in the postsynaptic active zones of both GABAergic and glutamatergic synapses already during the early postnatal period in mouse hippocampus. GABAergic terminals contained the α1 and β1 subunits of NOsGC, and a NO donor was able to induce cGMP production in these terminals, which effect was abolished by NOsGC inhibitors. In postnatal acute slices, NO was found to decrease GABAergic and glutamatergic postsynaptic currents (PSCs), whereas multineuron calcium imaging revealed that inhibition or stimulation of NO signaling enhanced or suppressed synchronous network events, respectively. These results provide the first evidence that the synapse-specific NO signaling machinery is present during the early postnatal days. By the reduction of GABAergic and glutamatergic synaptic transmission, it is able to fine-tune the first synaptic events and thereby affect synchronous network activity in the hippocampus at a time when GABAergic transmission is still depolarizing.

Materials and Methods

Animal Perfusions

All experiments were performed in accordance with the Institutional Ethical Codex and the Hungarian Act of Animal Care and Experimentation guidelines, which are in concert with the European Communities Council Directive of 24 November 1986 (86/609/EEC). Twenty-two male C57BL/6 mice between the ages of 4 days (P4) and 14 days (P14) in addition to 2 males and 1 female 6 days old (P6) nNOS knockout (–/–) mice were deeply anesthetized with isoflurane, followed by an intraperitoneal injection of 0.1–0.2 mL of an anesthetic mixture (containing 0.83% ketamine, 0.17% xylazin hydrochloride, 0.083% promethazinium chloride, 0.00083% benzethonium chloride, and 0.00067% hydrochinonum). Animals were perfused transcardially with 0.9% NaCl solution followed by a fixative. The perfusions were performed differentially depending on the type of immunocytochemistry that followed. In the preembedding experiments for localizing nNOS, the fixative contained 1% freshly depolymerized paraformaldehyde in 0.1 M phosphate buffer (PB), pH 7.4, and the animals were perfused for 60 min. In the preembedding experiments for localizing NOsGC subunits, the fixative contained 4% freshly depolymerized paraformaldehyde in 0.1 M PB, pH 7.4, and the animals were perfused for 40 min. All fixative solutions were followed by perfusion with 0.1 M PB for 10 min, the brains were removed from the skull and were not postfixed. Blocks containing the dorsal hippocampi were dissected and coronal sections were prepared on a Vibratome (VT1000S; Leica) at 70–100 μm, followed by washing in 0.1 M PB. Then, they were incubated in 10% and 30% sucrose in PB for cryoprotection, and freeze thawed over liquid nitrogen. After repeated washes in 0.1 M PB, the sections were processed for immunostaining.

Slice Preparation

For slice preparation, 5 to 8-day-old (P5–P8) animals were decapitated, the brains were removed and placed into ice-cold cutting solution containing the following (in mM): 252 sucrose, 2.5 KCl, 1.25 NaH_2PO_4, 5 $MgCl_2$, 0.5 $CaCl_2$, 26 $NaHCO_3$, and 10 glucose. The cutting solution had been bubbled with 95%O_2/5%CO_2 (carbogen gas). Coronal or horizontal hippocampal slices were prepared on a Vibratome (VT1200S; Leica). We prepared 300 μm thick slices for cGMP immunhistochemistry and 450 μm thick slices for the in vitro electrophysiology and multineuron calcium imaging experiments. Slices were incubated for 1 h in artificial cerebrospinal fluid (ACSF; in mM: 126 NaCl, 3.5 KCl, 1.25 NaH_2PO_4, 1.3 $MgCl_2$, 2 $CaCl_2$, 26 $NaHCO_3$, and 10 glucose) equilibrated with carbogen gas, at room temperature, in interface conditions before the experiments. For the electrophysiological and multineuron calcium imaging experiments, slices were transferred to submerged type dual-superfusion chambers (Hajos et al. 2009). For the cGMP immunohistochemistry experiments, slices were transferred to sterile 12-well cell-culture plates (TPP). Each well was filled with 1000 μL ACSF containing 1 mM 3-isobutyl-1-methylxanthine (IBMX) and 100 μM BAY-73 6691 to block phosphodiesterase (PDE) activity. Wells were individually bubbled with carbogen gas at equal rates. Slices from 3 animals were divided into control- (CTRL-), sodium nitroprusside- (SNP-), and oxadiazolo-quinoxaline-one (ODQ) + SNP-wells. No drugs were applied in the control wells, 10 μM ODQ was added to the ODQ + SNP-wells, and 30 min later 0.2 mM SNP was added to the SNP- and ODQ + SNP-wells. After SNP administration, slices were incubated for 10 more minutes. After incubation, the solutions were quickly changed to ice-cold 4% paraformaldehyde in 0.1 M PB, and then, the slices were postfixed in the same fixative for 48 h at 4 °C prior to immunohistochemistry.

Immunohistochemistry

For immunogold and combined immunogold–immunoperoxidase stainings, we incubated the sections in 1% human serum albumin (HSA; Sigma) diluted in tris-buffered saline (TBS), pH 7.4. Then, the sections were incubated for 60 h in the following solutions of primary antibodies diluted in TBS: 1) rabbit anti-nNOS 1:5000, 2) 1:400 (Zymed Laboratories, cat. no.: 61-7000), 3) rabbit anti-nNOS (1:400) combined with mouse anti-GAD65 (1:1000, Millipore, cat. no.: MAB351), 4) rabbit anti-NOsGC α1 (1:1000, Sigma-Aldrich, cat. no.: G4280) alone or combined with mouse anti-GAD65 (1:250), or 5) rabbit anti-NOsGC β1 (1:2000, Cayman Chemical, cat. no.: 160897) alone or combined with mouse anti-GAD65 (1:250). After repeated washes in TBS, sections were treated with blocking solution (Gel-BS) containing 0.5% cold water fish skin gelatin and 0.5% HSA in TBS for 1 h. This was followed by incubation in the following solutions of secondary antibodies diluted in Gel-BS for 24 h: 1) biotinylated donkey anti-rabbit (1:1000, Jackson ImmunoResearch Europe Ltd), 2) 1.4-nm gold-conjugated goat anti-rabbit (1:150, Fab' fragment, Nanoprobes), 3) 1.4-nm gold-conjugated goat anti-rabbit (1:150) combined with biotinylated donkey anti-mouse (1:1000, Jackson ImmunoResearch Europe Ltd), or 4) and 5) biotinylated donkey anti-rabbit (1:1000, Jackson ImmunoResearch Europe Ltd) alone or combined with 1-nm gold-conjugated goat anti-mouse (1:160, GE Healthcare). After intensive washes in TBS and 0.1 M PB, sections were treated with 2% glutaraldehyde in 0.1 M PB for 15 min to fix the gold particles into the tissue. In the combined method, this was followed by further washes in 0.1 M PB, TBS, and incubation in Elite ABC (1:300, Vector Laboratories) diluted in TBS. After this, sections were washed in TBS and tris-buffer at pH 7.6. The immunoperoxidase reaction was developed using 3,3-diaminobenzidine (DAB) as chromogen. After repeated washes in TBS and enhancement conditioning solution (Aurion), gold particles were intensified using the silver enhancement solution (Aurion) for 25–60 min at room temperature. After subsequent washes, sections were treated with 0.5% osmium tetroxide in PB for 20 min. Then, sections were dehydrated in ascending ethanol series and acetonitrile and embedded in epoxy resin (Durcupan, ACM, Fluka). During dehydration sections were treated with 1% uranyl acetate in 70% ethanol for 20 min.

For the electron microscopic investigations, small resin-embedded tissue samples were cut from the sections and glued onto plastic blocks. After this, 70 and 90-nm thick sections were cut using a Leica EM UC6 ultramicrotome and picked up on single-slot copper grids. The sections were examined using a Hitachi H-7100 electron microscope and a side-mounted Veleta CCD camera (Olympus Soft Imaging Solutions).

For the double immunofluorescent stainings, the slices were washed in PB, embedded in agar, resectioned into 50 μm thick sections on a Leica VT1000S Vibratome. After washes in PB and TBS containing 0.3% Triton X-100 (TBST; Sigma), sections were blocked for 45 min in 10% normal donkey serum (Vector Laboratories) dissolved in TBST. After this, sections were incubated for 48 h in a mixture of the following primary antibodies: sheep anti-cGMP (1:4000) and mouse anti-GAD65 (1:250) diluted in TBS. This was followed by washes in TBS and a 24 h incubation in biotinylated donkey anti-mouse (1:200) diluted in TBS. After subsequent washes in TBS, sections were incubated for 24 h in the mixture of the following secondary antibodies: Alexa Flour 488 donkey anti-sheep (1:200) and Alexa Fluor 594 streptavidin (1:200) diluted in TBS. This was followed by washes in TBS, PB, and the sections were mounted onto glass slides, coverslipped with Aquamount (BDH Chemicals Ltd). Immunofluorescence was analyzed using an Olympus Optical FluoView300 confocal laser scanning microscope in sequential scanning mode.

Great care was taken to test the specificity of the antibodies used in our work. The antibodies against nNOS was extensively tested before (Szabadits et al. 2007), and we also repeated these control experiments on fixed brain tissue from nNOS–/– P6 animals, where staining could not be observed. The antibodies, labeling the α1 and β1 subunits of NOsGC were extensively tested earlier in our laboratory (Szabadits et al. 2007), using colocalization and mRNA in situ hybridization experiments. The anti-GAD65 antibody was also characterized and its specificity was tested by other laboratories (Chang and Gottlieb 1988). The specificity of the antibody against cGMP was also tested (de Vente et al. 1987; Tanaka et al. 1997). Possible cross-reactions of secondary antibodies were also tested in several control experiments that confirmed the specificity of these antibodies as well.

In Vitro Electrophysiology

Whole-cell recordings were performed at 31–32 °C under visual guidance using Zeiss Axioscope. ACSF, equilibrated with 5% CO_2/95% O_2 gas, was superfused with the flow rate of 2–3 mL/min. Patch

electrodes had resistances of 3–6 MΩ when filled with the intracellular solution containing in mM: 80 CsCl, 60 Cs-gluconate, 1 $MgCl_2$, 2 Mg-ATP, 3 NaCl, 10 4-(2-hydroxyethyl)-1-piperazineethanesulfonic acid, 5 QX-314 (pH = 7.3, 290 mOsm). In some experiments, the pipette solution contained 0.1–0.3% biocytin, and post hoc morphological identification of recorded cells using an immunofluorescent method confirmed that these were all pyramidal neurons. PSCs were recorded at a holding potential of –70 mV. Slices were superfused with ACSF containing 2–3 mM kynurenic acid or 70–100 μM picrotoxin to block ionotropic glutamate receptors or $GABA_A$ receptors, respectively. Using a Supertech timer and isolator (Supertech Ltd, www.super-tech.eu), electrical stimulation of fibers was delivered in every 10 s (0.1 Hz) via a theta glass pipette (Sutter Instrument Company) filled with ACSF. To evoke glutamate receptor–mediated synaptic currents (GluR-PSCs) or $GABA_A$ receptor–mediated PSCs ($GABA_AR$-PSCs), the pipette was placed in the stratum radiatum (str. rad.) or in the str. pyramidale, respectively, in the CA1 region of the hippocampus. Access resistances (between 4–15 MΩ, compensated 65–70%) were frequently monitored and remained constant (±20%) during the period of recording. For statistical analysis, the Wilcoxon matched pair (WMP) test or the Mann–Whitney *U* test were used (OriginPro 8.0; OriginLab Corporation).

Multineuron Calcium Imaging

The recordings were performed at a flow rate of 8–10 mL/min, at 32–33 ^oC. Areas from CA1 str. pyramidale were loaded with the cell-permeant calcium indicator Fura-2 AM (20 μM) and pluronic acid (0.16% w/v) in ACSF, using a standard patch pipette (2–4 μm diameter) and a pressure microinjection system (Picospritzer, Narishige). Ratiometric imaging was performed using alternating excitation at 340 and 380-nm wavelengths with 100-ms exposure time, using a monochromator (TILL Photonics), while a CCD camera captured the emitted light (TILL Photonics). Five hundred images were taken during 155 s with 4 × 4 pixel binning (1 ratiometric frame/310 ms). Relative changes in Ca^{2+} levels were calculated from the ratio of the emitted fluorescent light in the 2 wavelengths (340 and 380 nm). Each active cell was marked manually as a region of interest (ROI), and the changes in the ratio during the measured periods were calculated in each ROI by the software (TILL Photonics). Events were considered synchronous, if Ca^{2+} signals increased simultaneously in more than 90% of the active cells. In all examined slices, we compared the number of active versus synchronous cells, and we found that at least 87% of the active cells participated in the synchronous events (SEs). The number of active cells recorded in one field of view was 15 ± 5 standard deviation (SD). After recording the control period, different drugs were bath applied to the slices for 10–12 min (100 μM N-omega-Nitro-L-Arginine-Methyl-Esther-Hydrochloride (L-NAME), 10 μM ODQ, 200 μM SNP, and 50 μM Br-cGMP), followed by the second recording to monitor the effects of the drugs on SEs. In every slice, we compared the number of SEs during the control period and after drug application.

In some cases, the activities of single cells were recorded simultaneously with the optical imaging of their Ca^{2+} changes. In these experiments, unit activity was recorded in loose patch mode, using patch pipettes (3–6 MΩ) filled with ACSF. All data were recorded with a Multiclamp 700B amplifier (Axon Instruments), filtered at 2 kHz, digitized at 10 kHz, and analyzed off-line with the EVAN program (courtesy of Prof. I. Mody, University of California, Los Angeles) and Origin 8.0 (OriginLab Corporation).

Drugs

L-NAME, SNP, and 8-Br-cGMP were dissolved in distilled water; IBMX, BAY-73 6691, and ODQ in dimethyl sulfoxide. Drugs were prepared as stock solutions and diluted to the required concentrations. Drugs were obtained from Tocris (www.tocris.com) or from Sigma (www.sigmaaldrich.com).

Although SNP was reported to have some side effects under certain conditions, its effect was always completely abolished by ODQ that is a potent and highly selective inhibitor of the cGMP-producing NO receptor (Garthwaite et al. 1995; Groneberg et al. 2008). In addition, the effect of the cGMP analogue, that mimics the effect of NO, was identical to the NO-donor SNP. Consequently, even if SNP had some side effects, under the physiological conditions used in our experiments they were undetectable, and the effects observed in our functional assays are due to the effect of NO (released by SNP) via the NO receptors.

Analysis

Because most data populations in this work did not have a Gaussian distribution according to the Shapiro–Wilk's *W* test, we used nonparametric statistics. Two independent groups were compared using the nonparametric Mann–Whitney *U* test; 2 dependent groups were compared using the nonparametric WMP test; the null hypothesis was rejected when the *P* level was under 0.05, and, in such cases, the differences were considered significant throughout this paper. In the electron microscopic experiments, terminals were considered to be GABAergic if they were GAD65 immunopositive, while terminals that were GAD65 immunonegative and established asymmetric synapses were considered to be glutamatergic. Indeed, post hoc analysis showed that GABAergic terminals, selected on the basis of these criteria, established significantly larger synapses than glutamatergic terminals (Mann–Whitney *U* test, $P < 0.01$). Furthermore, the postsynaptic profiles of GABAergic terminals were larger than those postsynaptic to glutamatergic boutons that is also expected because of the size difference between dendritic shafts and spines.

Results

nNOS Is Associated with the Postsynaptic Active Zones of GABAergic and Glutamatergic Synapses in the Developing Hippocampus

Since synchronous neuronal activity is a characteristic phenomenon of developing cortical networks that is most prominent around postnatal day 6 in mice (Crepel et al. 2007; Allène et al. 2008), when GABAergic transmission is still depolarizing, we focused most of our experiments to investigate this developmental stage. We localized nNOS during these early postnatal days and performed single and double immunogold–immunoperoxidase stainings for nNOS and GAD65 on wild type (WT) and nNOS–/– mice. In the single immunoreactions for nNOS in the P6 WT mice, the pyramidal cells were stained weakly, and some strongly immunopositive interneurons were detected in the CA1 and CA3 areas. In nNOS–/– mice, no labeling was found. In the region of the synaptic active zones, the immunogold-labeling pattern for nNOS was identical in mice at P4 (Fig. 1*E,F*), P6 (Fig. 1*A–C*), P10, and P14. Mostly postsynaptic densities were labeled in the hippocampal CA1 and CA3 areas, with some labeling also associated with extrasynaptic cell membranes, and a few gold particles localized on intracellular membrane organelles close to synapses. The linear density of the nNOS labeling was 1.36 gold particles/μm in the synapses (median, 0.7–1.37 min–max, 3 mice) and 0.06 gold particles/μm extrasynaptically (median, 0.06–0.07 min–max, 3 mice, Fig. 3*E*), while in the nNOS–/– mice, no such labeling was detected. A remarkable 46% of the fully reconstructed randomly sampled synapses from str. rad. of CA1 of P6 mice were labeled for nNOS (median, 41–50% min–max; $n = 66$ synapses in 3 mice, Fig. 3*A*).

Using GAD65 labeling and other morphological criteria (see Materials and Methods), we identified GABAergic and glutamatergic terminals and found that postsynaptic nNOS immunolabeling was present in both types of synapses in the CA1 and CA3 regions of P4 (Fig. 1*E,F*), P6 (Fig. 1*B,C*), P10, and P14 mice. We found that 40% of GABAergic (median, 27–47% min–max; $n = 45$ synapses in 3 P6 mice) and 33% of glutamatergic (median, 29–40% min-max; $n = 44$ synapses in 3 P6 mice) fully

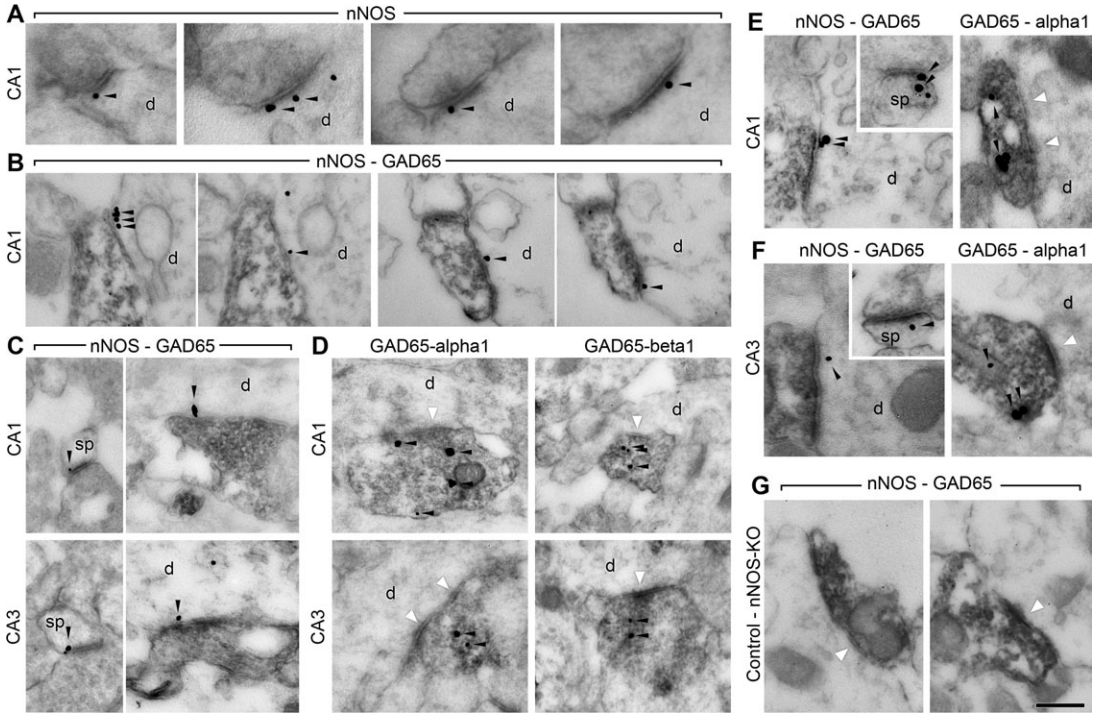

Figure 1. The molecular elements of the retrograde NO-signaling pathway are present at GABAergic and glutamatergic synapses in the developing hippocampus at P4 and P6. (*A*) Electron micrographs show immunogold labeling for nNOS in the postsynaptic active zones of dendritic synapses. (*B*) Two image series show postsynaptic nNOS immunogold labeling in synapses made by GAD65-positive (dark DAB precipitate) axon terminals. (*C*) Electron micrographs show that nNOS is present postsynaptically in GABAergic synapses on dendritic shafts and in glutamatergic synapses on spines in the CA1 and CA3 regions of the hippocampus. (*D*) Images show double immunohistochemical reactions for either NOsGC α1 or β1 (dark DAB precipitate) combined with GAD65 (intensified gold particles). Both subunits of the NO receptor are present in GABAergic synaptic axon terminals in the CA1 and CA3 areas. (*E,F*) The labeling patterns were identical in mice at P4 in the CA1 and CA3 areas (see above). (*G*) Photos demonstrate a complete lack of nNOS immunolabeling in the knockout animals, in the nNOS-GAD65 double-labeling experiments. Scale bar is 200 nm for *A* and 300 nm for *B–F*. Black arrowheads point to the intensified immunogold particles, white arrowheads show synapses. Spines (sp), dendrite shafts (d).

reconstructed synapses expressed nNOS postsynaptically (Fig. 3*B,C*).

Both α1 and β1 Subunits of the NO receptor Are Present in GABAergic Axon Terminals during Development

In order to examine the subcellular distribution of α1 and β1 subunits of NOsGC, we performed single and double stainings for these subunits alone or in combination with GAD65.

The α1 subunit labeling of P4–P14 mice was similar to the developmental labeling pattern described for GAD (Dupuy and Houser 1996), suggesting that it labels mostly GABAergic terminals. Unlike pyramidal cells in the CA1 and CA3 areas, interneuron somata were α1 subunit immunopositive, along with a dense meshwork of axonal fibers and terminals localized predominantly in the str. rad. at P4–P10. At P14 the labeling was weaker but similar to the adult pattern (Szabadits et al. 2007), that is, the cell bodies of interneurons were labeled in all layers and their axon terminals were also α1 subunit positive, especially in the str. pyramidale. In the adult hippocampus, both in situ hybridization and immunohistochemical experiments showed that the α1β1 subunit composition of the NO receptor is interneuron specific (Szabadits et al. 2007), and indeed, unlike pyramidal cells in the CA1 and CA3 areas, interneuron somata were α1 subunit immunopositive at P4–P10. In addition, we found that α1 subunit–positive terminals always made symmetric synapses, and never asymmetric ones nor did they contact spines or spine-like structures at any ages examined. These data suggests that most if not all α1+ terminals are GABAergic already during development, and indeed, in the double-labeling experiments, we frequently found synaptic terminals positive for both GAD65 and α1 subunits in the CA1 and CA3 regions at P4 (Fig. 1*E,F*), P6 (Fig. 1*D*), P10, and P14 ages. Fifty-four percent (median, 53–57% min–max; n = 88 synapses in 3 P6 mice) of the reconstructed, randomly sampled GAD65-positive synaptic terminals in CA1 were positive for the α1 subunit (Fig. 3*D*).

The β1 subunit labeling was similar to the adult pattern. Pyramidal cells showed weak cytoplasmic staining, and the neuropil showed a diffuse, punctate labeling. Interneuron somata and immunopositive axon terminals were stained for β1 subunit as early as P4–P6. The β1 subunit–containing axon terminals formed symmetric synapses. In the double-immunostained preparations, GAD65 and β1 subunit double-positive axon terminals formed synapses in the str. rad. of CA1 and CA3 regions from P4, P6 (Fig. 1*D*), P10, and P14 mice.

These results show that the NOsGC α1β1 subunit composition is present in GABAergic terminals during postnatal development, and it is in an ideal position to receive retrograde NO signal synthesized in the postsynaptic compartment by nNOS.

Activation of the NO Receptor Induces cGMP Production in GABAergic Axon Terminals of the Developing Hippocampus

To test whether the NO receptor is functional during the early postnatal days, we prepared acute hippocampal slices from P6

mice, incubated them in oxygenated ACSF containing PDE inhibitors, and treated them either with no drugs, with the NO-donor SNP (200 μM), or with a selective inhibitor of the NO receptor (ODQ, 10 μM), followed by the addition of the NO donor (Fig. 2*A*). These incubations were followed by fixation and double immunofluorescent labeling for GAD65 and cGMP. After incubation with no drugs (control conditions), we did not find labeled terminals in the randomly collected samples (Fig 2*A*—CTRL), but some glia-like cGMP immunoreactivity could be detected in these control hippocampal slices. After NO-donor (SNP) treatment, strongly cGMP-immunopositive fibers and terminals could be observed (Fig 2*A*—SNP) along with a few labeled neuronal somata and some glia-like staining. After pretreatment with ODQ, SNP could not induce any detectable cGMP signal (Fig. 2*A*—ODQ + SNP). In the SNP-treated slices, we found that 28% (median, 23–34% min–max; n = 508 terminals in 3 mice) of the randomly sampled GAD65-positive terminals of the str. rad. showed cGMP immunoreactivity, and at least 41% (median, 39–41% min–max; n = 335 terminals in 3 P6 mice, Fig. 2*B*) of the cGMP-positive terminals were positive for GAD65 (Fig. 3*F*,*G*). Therefore, NOsGC is able to produce cGMP in these terminals already during the first postnatal days.

NO Decreases both GABAergic and Glutamatergic Postsynaptic Currents in a NOsGC-Dependent Manner

Using a whole-cell patch-clamp method, we recorded evoked PSCs in CA1 pyramidal cells in slice preparations from P5–P8 mice. First, we examined the effect of the NO donor, SNP (200 μM) on the amplitude of pharmacologically isolated $GABA_A$R-PSCs, evoked by electrical stimulation in the str. pyramidale. Application of SNP significantly decreased the peak amplitude of $GABA_A$R-PSCs to 67% of control values (control median amplitude: 186.5 pA and interquartile range: 149.2–240.8 pA; median amplitude in SNP: 125.6 pA and interquartile range: 92.8–184.8 pA, n = 12 slices, P = 0.00097, WMP test, Fig. 4*A*–*C*). The sensitivity of $GABA_A$R-PSCs to SNP was not homogenous. In the majority of cases, SNP reduced the amplitude of events significantly to 52% of control (control median amplitude: 231.7 pA and interquartile range: 161.6–443.9 pA; median amplitude in SNP: 120.3 pA and interquartile range: 56.1–329.6 pA, n = 7 slices, P = 0.015, WMP test). In the other cases, SNP caused no significant change in the peak amplitude (control median amplitude: 151.3 pA and interquartile range: 142.7–180.9 pA; median amplitude in SNP: 137.6 pA and interquartile range: 126.8-–77.2 pA, n = 5 slices, P = 0.12, WMP test). We then tested whether the suppressing effect was mediated by NOsGC. We pretreated slices with ODQ, the blocker of NOsGC, followed by coapplication of ODQ and SNP. After the control period, we bath-applied 10 μM ODQ, which caused a small reduction in the peak amplitudes of $GABA_A$R-PSCs (control median amplitude: 130.8 pA and interquartile range. 92.8–226.2 pA; median amplitude in ODQ: 99.5 pA and interquartile range: 50.2–171.8 pA, n = 9 slices, P = 0.004, WMP test). Then, we treated the slices with SNP in the presence of ODQ. In all but one instance, SNP could not reduce the amplitude (median amplitude in ODQ: 132.3 pA and and interquartile range: 63.3–194.2 pA; median amplitude in SNP + ODQ: 131.8 pA and interquartile range: 56.7–181.4 pA, n = 8 slices, P = 0.25, WMP test, Fig. 4*D*–*F*). The comparison of the control peak amplitudes of $GABA_A$R-PSCs before application of drugs in the 2 sets of experiments (SNP experiments [control: 186.5 pA] or ODQ + SNP experiments [control: 130.8 pA]) revealed no significant difference (P = 0.18, Mann–Whitney U test), suggesting that similar sets of GABAergic fibers were

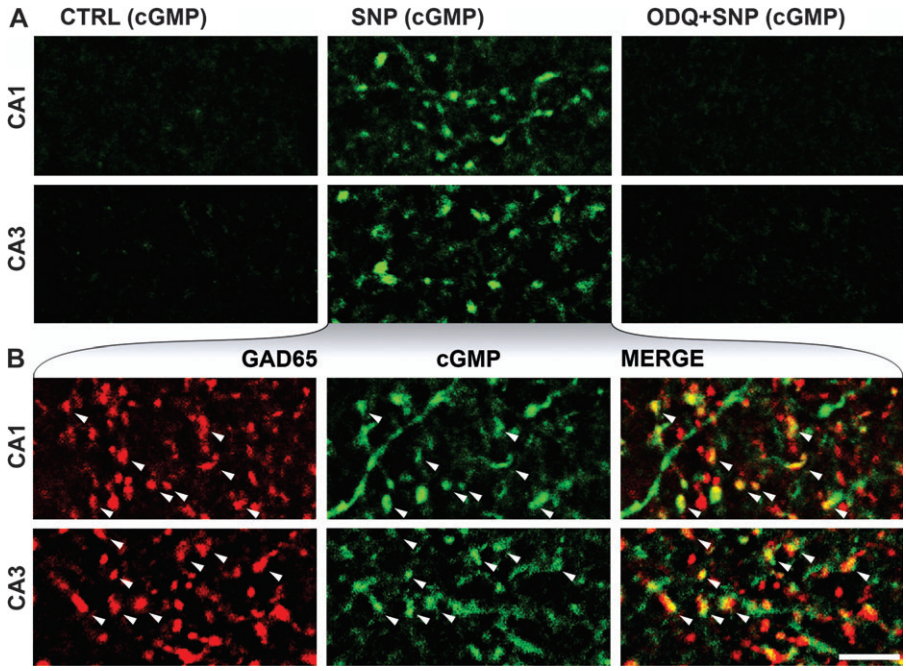

Figure 2. NO donor (SNP) induces cGMP production in a NO receptor–dependent manner in axon terminals during development. (*A*) Confocal laser scanning images show immunofluorescent cGMP labeling in the str. rad. of the hippocampus of P6 mice. In the presence of PDE inhibitors, slices were pretreated with: no drugs (CTRL), the NO-donor SNP, or the NO-receptor blocker ODQ, followed by SNP (ODQ + SNP). No terminals were labeled for cGMP in the randomly collected samples from the CTRL experiments (first column). SNP-induced cGMP production in the CA1 and CA3 areas (SNP, second column) was completely blocked by ODQ (ODQ + SNP, third column). (*B*) Colocalization of GAD65 and cGMP immunoreactivity in the NO donor–treated slices in the CA1 and CA3 areas (str. rad. of P6 mice). White arrowheads show some terminals that have cGMP and GAD65 immunoreactivity. Scale bar: 5 μm for all images.

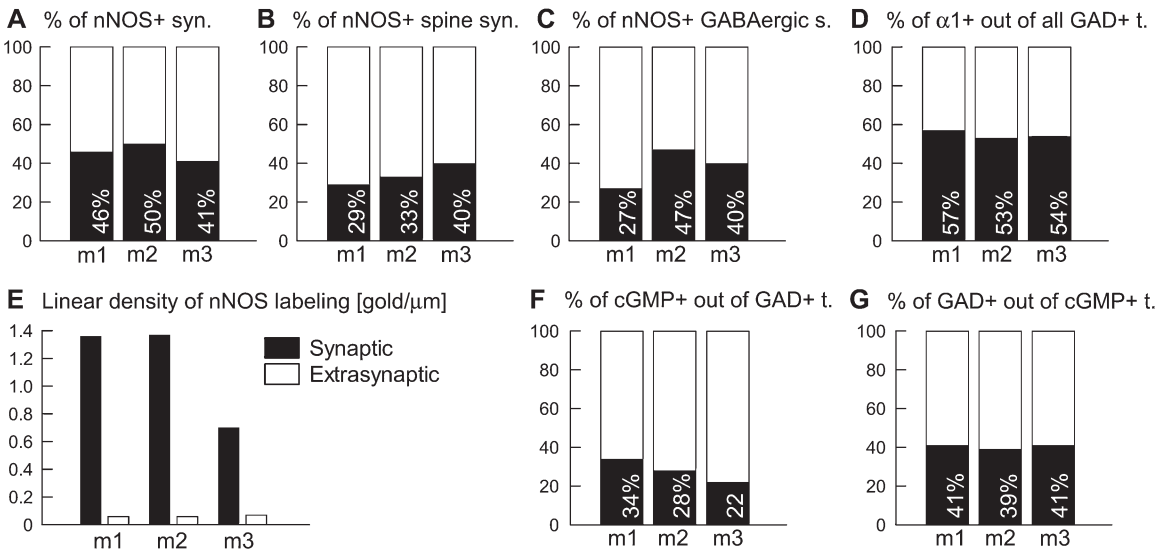

Figure 3. Analysis of the distribution of NO-signaling molecules during postnatal development in 3 P6 mice (m1, m2, and m3). (*A*) The percentage of nNOS-positive synapses of all identified synapses ($n = 66$) from single-labeling experiments. (*B*,*C*) In double-labeling experiments, we also tested glutamatergic and GABAergic synapses separately. The graphs show the percentages of nNOS-positive synapses of all glutamatergic synapses (*B*, $n = 44$) and of all GAD65-positive synapses (*C*, $n = 45$). (*D*) The percentage of NOsGC α1-positive synapses of all GAD65-positive terminals ($n = 88$). (*E*) The linear density of immunogold particles along the cell membrane for nNOS was 1.36 gold/μm in synapses (median, 0.7–1.37 min–max) and 0.06 gold/μm on extrasynaptic membranes (median, 0.06–0.07 min–max) tested on electron microscopic images (from 32 μm synaptic and 604 μm extrasynaptic membrane segments). (*F*) The percentage of cGMP-positive terminals of all GAD65-positive terminals ($n = 508$). (*G*) The percentage of GAD65-positive terminals of all cGMP labeled terminals ($n = 335$).

stimulated in both experiments. These results showed that NO can control the efficacy of GABAergic synaptic transmission via activation of NOsGC.

Next, we investigated the impact of NO on glutamatergic transmission as well. First, we tested the effect of SNP on the peak amplitude of pharmacologically isolated ionotropic GluR-PSCs evoked by focal stimulation in the str. rad. Application of SNP invariably reduced the GluR-PSC amplitude by half (control median amplitude: 63.2 pA and interquartile range: 26.1–104.9 pA; median amplitude in SNP: 30.58 pA and interquartile range: 9.1–60.5 pA, $n = 7$ slices, $P = 0.015$, WMP test, Fig. 5*A–C*). Next, we pretreated the slices with ODQ, which in itself did not alter significantly the peak amplitude (control median amplitude: 42.8 pA and interquartile range: 24.3–120.6 pA; median amplitude in ODQ: 37.9 pA and interquartile range: 30.5–69.6 pA, $n = 7$ slices, $P = 0.57$, WMP test) but again occluded the effect of SNP (median amplitude in SNP + ODQ: 31.1 pA and interquartile range: 25.2–70.1 pA, $n = 7$ slices, $P = 0.22$, WMP test, Fig. 5*D–F*). The control amplitudes of GluR-PSCs were similar in both sets of experiments ($P = 0.79$, Mann–Whitney *U* test). These data show that the glutamatergic synaptic communication is also depressed by NO signaling via NOsGC in postnatal hippocampal slices.

Modulation of NO Signaling Alters Synchronous Network Activity in Developing Hippocampal Slices

To test whether NO signaling can influence synapse-driven synchronous network activity, we used multineuron calcium imaging in acute hippocampal slices. Areas from CA1 str. pyramidale were loaded with the calcium indicator Fura-2 AM (20 μM, Fig. 6*A*). In control conditions, simultaneous calcium imaging and recording of the unit activity of the same cell in loose patch mode revealed that the calcium elevations corresponded to burst firings of the same cells (Fig. 6*B,C*). The number of SEs during recordings (155 s) was 8.6 ± 4.7 SD ($n = 26$ slices).

Then, we examined the effect of pharmacological blockade of the NO signaling on the occurrence of SEs. The NOS inhibitor L-NAME (100 μM) significantly increased the number of SEs to 157% of control in WT (median, 145–700% min–max; $P = 0.0117$, WMP test; $n = 8$ slices, in 4 mice, Fig. 6*D,E*) but not in nNOS–/– mice (see Fig. 6*E*, $n = 3$, in 3 mice, open circles with dashed lines). Similarly, the NO-receptor inhibitor ODQ (10 μM) also increased the number of SEs significantly to 356.6% of control (median, 178–583% min–max; $P = 0.0277$, WMP test; $n = 6$, in 3 mice, Fig. 6*F,G*). These results indicated that there was a basal NO signaling in the network that restrained the synapse-driven SEs.

Stimulation of the NO-signaling pathway was also tested. We bath applied either the NO-donor SNP (200 μM) or the membrane-permeable cGMP-analogue Br-cGMP (50 μM). These drugs significantly decreased the number of SEs to 15.5% of the control (median, 0–31% min-max; $P = 0.0277$, WMP test; $n = 6$, in 4 mice, Fig. 6*H,I*) or to 41% of control (median, 17–60% min–max; $P = 0.0277$, WMP test; $n = 6$, in 3 mice, Fig. 6*J,K*), respectively. The effect of Br-cGMP could be completely washed out in 4 of 6 slices (2 slices were not tested). Thus, modulation of NO signaling can have a strong influence on hippocampal synchronous activity in early stages of development.

Discussion

Here, we investigated the NO signaling system in the mouse hippocampus during the early postnatal days, when the first synapse-driven synchronous network activity occurs. Our major findings are that 1) nNOS is present postsynaptically both in GABAergic and in glutamatergic synapses, 2) both α1 and β1 subunits of the NO receptor are expressed in

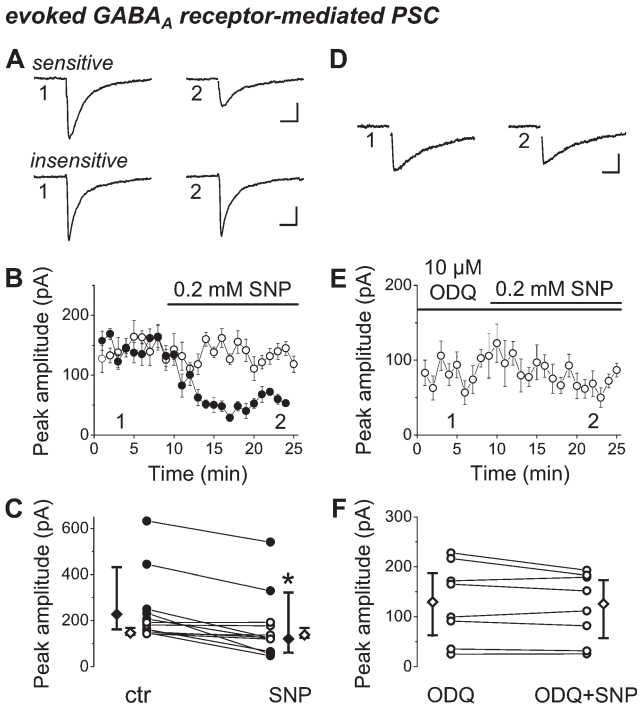

Figure 4. NO signaling suppresses GABAergic synaptic transmission in the developing hippocampus. (*A–C*) The NO donor SNP significantly decreased the peak amplitude of evoked $GABA_A$ receptor–mediated PSCs compared with control. On *A*,*B*, averaged events of 6–8 consecutive records were taken at the labeled time points. SNP either reduced the amplitude of events significantly (sensitive, filled circles) or caused no change in the peak amplitude (insensitive, empty circles). (*D–F*) Slices were pretreated with the NOsGC blocker ODQ, followed by coapplication of ODQ and SNP. ODQ abolished the effect of the NO donor. On *D*,*E*, averaged events of 6–8 consecutive records were taken at the labeled time points. For clarity, stimulus artifacts were removed from the averaged traces. *C* and *F* show changes of peak amplitude in individual slices. (*C*,*F*) The vertical bars adjacent to the pairwise comparisons indicate medians and interquartile ranges of the corresponding data (filled or empty symbols). The asterisk indicates significant difference (at $P < 0.05$). Scale bars; *A*,*D*: 20 ms, 40 pA; *B*,*E*: data shown as mean ± standard error of the mean (SEM).

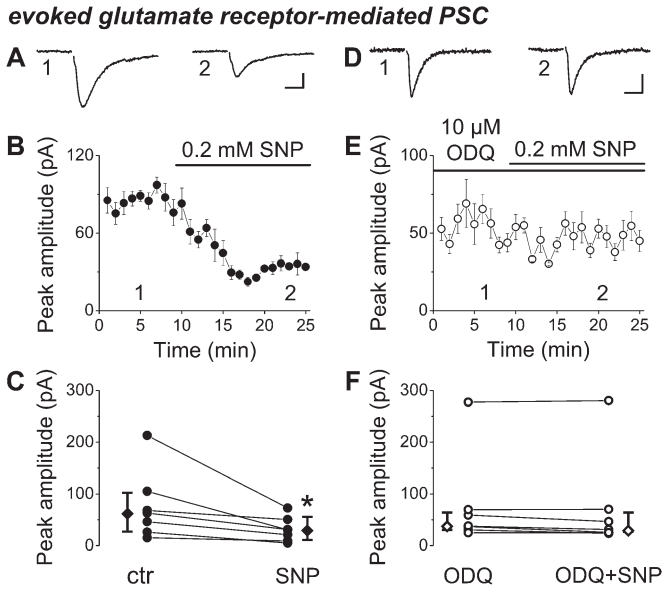

Figure 5. NO signaling suppresses glutamatergic synaptic transmission in the developing hippocampus. (*A–C*) The NO donor SNP invariably reduced the peak amplitude of ionotropic glutamate receptor–mediated synaptic currents compared with control. On *A*,*B*, averaged events of 6–8 consecutive records were taken at the labeled time points. (*D–F*) Slices were pretreated with the NOsGC blocker ODQ, followed by coapplication of ODQ and SNP. ODQ abolished the effect of the NO donor. On *D*,*E*, averaged events of 6–8 consecutive records were taken at the labeled time points. For clarity, stimulus artifacts were removed from the averaged traces. *C* and *F* show changes of peak amplitude in individual slices. (*C*,*F*) The vertical bars adjacent to the pairwise comparisons indicate medians and interquartile ranges. The asterisk indicates significant difference (at $P < 0.05$). Scale bars; *A*,*D*: 10 ms, 20 pA. *B*,*E*: data shown as mean ± SEM.

GABAergic axon terminals, 3) NO receptor is functional, as it can produce cGMP after NO stimulation, 4) NO signaling reduces the amplitude of GABAergic and glutamatergic synaptic currents, and 5) NO signaling is able to regulate synchronous network activity.

Synapse-specific NO production during development

nNOS is activated by Ca^{2+}–calmodulin complex under conditions of elevated intracellular Ca^{2+}concentrations (Prast and Philippu 2001). In the mature brain, this elevation can be generated by the activation of NMDA receptors at excitatory synapses, and other mechanisms also exist at GABAergic synapses (Makara et al. 2007; Szabadits et al. 2007). During early postnatal development, depolarizing effects of GABA lead to the activation of postsynaptic voltage-dependent calcium channels around GABAergic synapses (Eilers et al. 2001; Kullmann and Kandler 2008). This locally generated elevation of Ca^{2+} concentration may activate nNOS that we showed to be present in these synapses.

NO can freely cross membranes and is detectable only a few micrometers around its site of production (Namiki et al. 2005). The concentration of NO remains effective up to a few hundred nanometers away from the site of production (Garthwaite 2008). Activation of NOsGC is highly effective (Koesling et al. 2004), and deactivation is unexpectedly fast (Bellamy et al. 2000). These properties suggest an effective feedback pathway with a high spatial and temporal resolution. Our results show that nNOS is enriched not only in glutamatergic but also in GABAergic synapses, while the functional NO receptor is present presynaptically. This synapse-specific arrangement suggests that individual synapses or a small subset of them can be differentially modulated by retrograde NO signal.

NO signaling plays an important role in neuronal morphogenesis affects growth cones (Nikonenko et al. 2003), axonal guidance (Murray et al. 2009), and NO promotes synapse formation and stabilization as well (Nikonenko et al. 2008). In addition, NO may also act via nitrosylating other proteins, whereby it is able to modulate dendrite growth during neuronal development (Zhang et al. 2010). We found that nNOS was mostly localized in the postsynaptic densities of different synapses; but the remaining labeling was mainly on the cell membrane, from where it can diffuse to potential presynaptic targets. Therefore, it seems that after NO contributed to the establishment of functional synapses, the complete signaling pathway is in place to modulate vesicle release in GABAergic and glutamatergic synapses and to regulate network activity efficiently.

NO-Induced Presynaptic cGMP Production in Development

The NO-receptor NOsGC is present in the brain in 2 different subunit compositions, as $\alpha1\beta1$ and $\alpha2\beta1$. In the adult

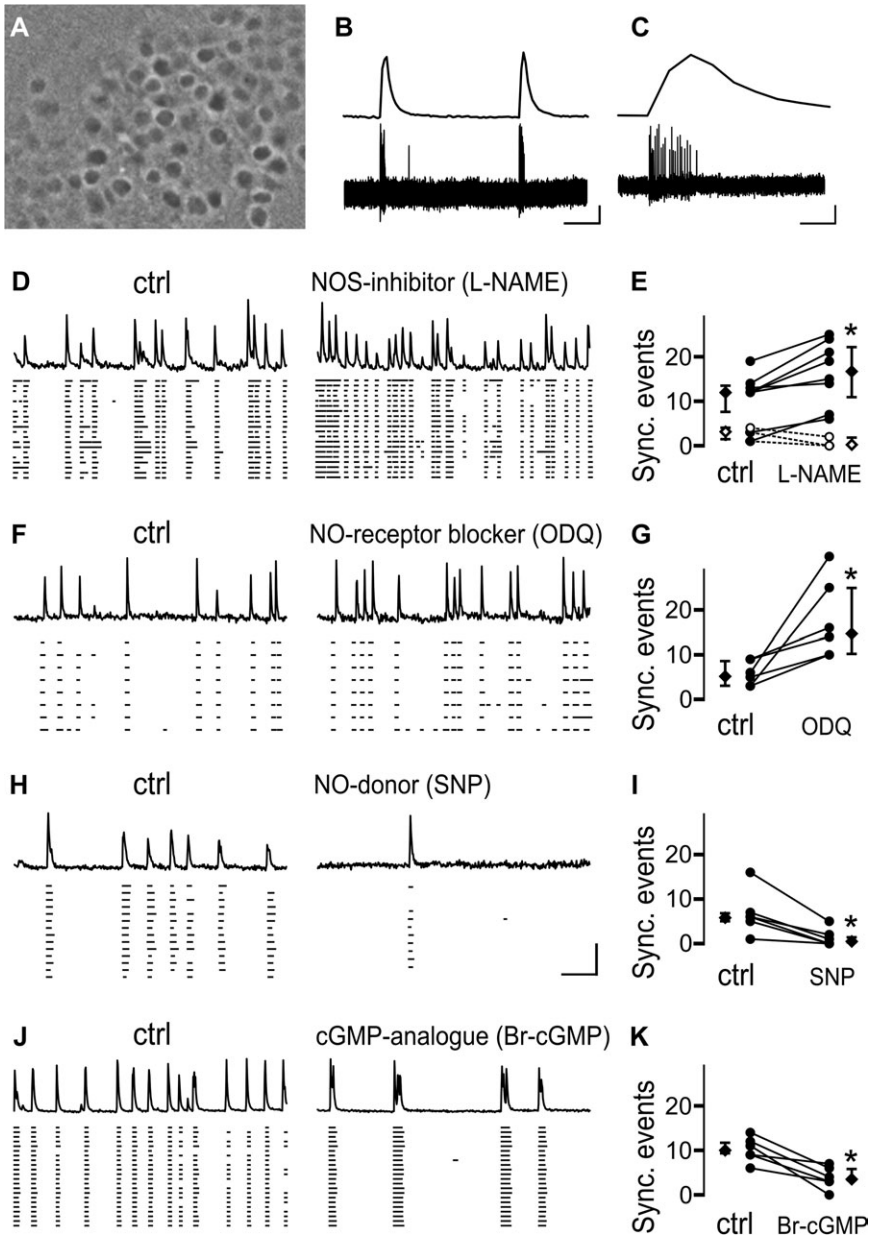

Figure 6. NO-signaling pathway can modulate the occurrence of SEs in acute hippocampal slices of 5–8 days old mice. (*A*) One representative frame of a movie, showing Fura-2 AM loaded pyramidal cells in the CA1 area. (*B*,*C*) Simultaneously recorded action potentials (lower trace) and ratiometric Ca^{2+} signal (upper trace) of the same cell. Unit activity was recorded extracellularly in a loose patch mode. The peaks in the fluorescence signal corresponded to burst firings of the same neurons. Scale bars: 5 s for *B*, 0.5 s for C, 0.1 mA, and 110 F340/F380 for both. (*D*,*F*,*H*,*J*) SEs in acute hippocampal slices. Left panels show basal activities, right panels show activities after drug application in the same slice preparation. The upper traces show the ratiometric Ca^{2+} signals of a representative cell and the raster plots under the traces correspond to the Ca^{2+} peaks of cells that participated in SE. Each row represents one cell, before and after drug application. Scale bar in *H* applies for *D*,*F*, and *J* as well, the horizontal bar is 20 s, and the vertical bar is 100, 140, 140, and 250 F340/F380 for *D*,*F*,*H* and *J*, respectively. (*E*,*G*,*I*,*K*) Number of SEs per 155 s under control conditions and after drug application. The vertical bars adjacent to the pairwise comparisons indicate medians and interquartile ranges of the corresponding data (filled or empty symbols). The asterisk indicates significant difference (at $P < 0.05$). Note that the number of SEs changed in the same direction in each slice treated with the same drug. (*D*,*E*) The NOS inhibitor L-NAME elevated the number of SEs in the WT (filled circles) but not in the nNOS−/− mice (empty circles with dashed lines). (*F*,*G*) ODQ increased the number of SEs. (*H*–*K*) SNP and Br-cGMP reduced the number of SEs.

hippocampus, α1β1 is interneuron specific, while the α2β1 composition is restricted to principal cells (Szabadits et al. 2007). Similarly, we found α1 subunits only in interneurons, while the β1 subunit was present also in pyramidal cells. We found NO receptors in GABAergic terminals during development. The lack of immunostaining for the β1 subunit in glutamatergic terminals could be due to lower protein levels in these smaller terminals or to the possible epitope masking of the α2-containing receptors by specific anchoring proteins, since these synapses could be also controlled by NOsGC activity (present study).

The activation of NOsGC by NO leads to the formation of the second messenger cGMP. Our results show that cGMP is produced in GABAergic (GAD65 positive) terminals, and it is mediated exclusively by the NO receptor because its inhibition (by ODQ) diminished the cGMP signal. The incomplete overlap between GAD65 and cGMP immunoreactivity suggests that cGMP production may be present in glutamatergic terminals,

fibers, or growth cones and filopodia as well. However, we cannot rule out the presence of some cGMP-containing GABAergic terminals that were false immunonegative for GAD65 due to technical reasons.

cGMP exerts its effects mainly via 3 molecular pathways, the PDEs, cyclic nucleotide-gated ion channels (CNG channels), and cGMP-dependent protein kinases (PKGs). In pyramidal cells and interneurons, PDE 2 and 9 can be detected from P0, while PDE 5 was found from P5 (Van Staveren et al. 2003). CNG channel expression was detected before synapse formation (Zufall et al. 1997), and there is a prominent expression of PKGs, observed from embryonic day 13.5 (Demyanenko et al. 2005). These data show that neurons are well equipped to process the NO-induced cGMP signal already during early postnatal development.

Synaptic NO-Signaling Controls both Glutamatergic and GABAergic Transmission and May Regulate Developmental Network Activity

The activation of NO signaling can increase or decrease transmitter release from different or even from the very same terminals under different conditions (Garthwaite 2008). Similar to our results, in the adult hippocampus, NO can act presynaptically to reduce glutamate (Prast and Philippu 2001) or GABA release (Makara et al. 2007). We showed that NO signaling depressed both GABAergic and glutamatergic synaptic transmission during the early postnatal period in a NO receptor–dependent manner. Because NO receptors were found in presynaptic terminals, the reduction of the amplitude of GABAergic synaptic currents is likely caused by the modulation of presynaptic transmitter release. The distinct NO sensitivity of different GABAergic connections found in the present study could be due to activity-dependent dynamic regulation of this signaling pathway, which may depend on the level of maturation or the type of interneurons involved.

Synchronous network activity is a hallmark of developing neuronal circuits (Ben-Ari et al. 2007; Blankenship and Feller 2010). The depolarizing GABAergic transmission is crucial for the emergence of this pattern in rodents (Sipila et al. 2006), primates (Khazipov et al. 2001), and in the human brain (Dzhala et al. 2005; Vanhatalo et al. 2005). The temporally patterned output of GABAergic interneurons and the intrinsic bursting activity of pyramidal cells have also been shown to be involved in the generation of synchronous network activities during development (Sipila et al. 2005; Bonifazi et al. 2009).

Using multineuron calcium imaging, we investigated the involvement of NO signaling in these activity patterns. We propose that retrograde NO signaling may alter the efficiency of transmission in a synapse-specific manner by modulating GABAergic and glutamatergic synapses via the NOsGC–cGMP pathway. Network synchrony in these animals is sustained by a large population of neurons via synaptic connections (Crepel et al. 2007; Bonifazi et al. 2009). Our results, showing that synchronous network activity can be modulated in vitro by exogenously applied blockers of the NO signaling pathway, suggest that this signaling is active in a large number of synapses during these SEs.

When synchronous burst activities depolarize pyramidal cells, nNOS can be activated synaptically by raising Ca^{2+} concentration, and NO receptor activation can become maximal. This is mimicked by the application of the NO donor or the cGMP analogue that in turn significantly decreased the number of SEs in our experiments. Our results also demonstrated that the pharmacological blockade of the retrograde NO-cGMP pathway at different stages significantly elevated the frequency of these SEs, indicating that under these physiological conditions, there is a basal NO-signaling activity. This suggests that NO signaling can restrain ongoing synchronous activity, thus protecting the network from hyperactivity.

During the first 2 postnatal weeks, feedback mechanisms are needed to stabilize network activities produced by synchronous discharges of large neuronal ensembles. Such mechanisms may engage presynaptic $GABA_B$ autoreceptors, which have been implicated in the control of SEs during development (McLean et al. 1996). Endocannabinoid signaling represents another system that can suppress release from a subset of GABAergic interneurons but in this case, the effect depends on postsynaptic activity and Ca^{2+} transients (Bernard et al. 2005). NO signaling is also retrograde, because it is triggered by postsynaptic Ca^{2+} transients and NO formation, but unlike endocannabinoids, it is not restricted to synapses formed by a particular subpopulation of interneurons. In addition, here we described that it can affect both GABAergic and glutamatergic signaling during development. Therefore, NO is ideally suited to fulfill a general feedback role that modulates synchronous network activity patterns during development.

Funding

Howard Hughes Medical Institute International Program; European Union (LSHM-CT-2004-005166); Nemzeti Kutatási és Technológiai Hivatal–Országos Tudományos Kutatási Alapprogramok (CNK77793, OMFB-01678/2009); Országos Tudományos Kutatási Alapprogramok (NNF 78917); National Institutes of Health (DA09158, MH54671, NS030549); and Wellcome Trust to N.H. János Bolyai Research Fellowship to G.N.

Notes

We thank Gergely Szabó for the help with the multineuron calcium imaging. The technical assistance of Gábor Patkovics, Katalin Lengyel, Katalin Iványi, Erzsébet Gregori, and Győző Goda is also greatly acknowledged. *Conflict of Interest*: None declared.

References

Akerman CJ, Cline HT. 2007. Refining the roles of GABAergic signaling during neural circuit formation. Trends Neurosci. 30:382–389.

Allène C, Cattani A, Ackman J, Bonifazi P, Aniksztejn L, Ben-Ari Y, Cossart R. 2008. Sequential generation of two distinct synapse-driven network patterns in developing neocortex. J Neurosci. 28:12851–12863.

Bellamy TC, Wood J, Goodwin DA, Garthwaite J. 2000. Rapid desensitization of the nitric oxide receptor, soluble guanylyl cyclase, underlies diversity of cellular cGMP responses. Proc Natl Acad Sci U S A. 97:2928–2933.

Ben-Ari Y, Gaiarsa JL, Tyzio R, Khazipov R. 2007. GABA: a pioneer transmitter that excites immature neurons and generates primitive oscillations. Physiol Rev. 87:1215–1284.

Bernard C, Milh M, Morozov YM, Ben-Ari Y, Freund TF, Gozlan H. 2005. Altering cannabinoid signaling during development disrupts neuronal activity. Proc Natl Acad Sci U S A. 102:9388–9393.

Blankenship A, Feller M. 2010. Mechanisms underlying spontaneous patterned activity in developing neural circuits. Nat Rev Neurosci. 11:18–29.

Bon CL, Garthwaite J. 2003. On the role of nitric oxide in hippocampal long-term potentiation. J Neurosci. 23:1941–1948.
Bonifazi P, Goldin M, Picardo MA, Jorquera I, Cattani A, Bianconi G, Represa A, Ben-Ari Y, Cossart R. 2009. GABAergic hub neurons orchestrate synchrony in developing hippocampal networks. Science. 326:1419–1424.
Burette A, Zabel U, Weinberg RJ, Schmidt HH, Valtschanoff JG. 2002. Synaptic localization of nitric oxide synthase and soluble guanylyl cyclase in the hippocampus. J Neurosci. 22:8961–8970.
Cancedda L, Fiumelli H, Chen K, Poo MM. 2007. Excitatory GABA action is essential for morphological maturation of cortical neurons in vivo. J Neurosci. 27:5224–5235.
Chang YC, Gottlieb DI. 1988. Characterization of the proteins purified with monoclonal antibodies to glutamic acid decarboxylase. J Neurosci. 8:2123–2130.
Chung YH, Kim YS, Lee WB. 2004. Distribution of neuronal nitric oxide synthase-immunoreactive neurons in the cerebral cortex and hippocampus during postnatal development. J Mol Histol. 35:765–770.
Crepel V, Aronov D, Jorquera I, Represa A, Ben-Ari Y, Cossart R. 2007. A parturition-associated nonsynaptic coherent activity pattern in the developing hippocampus. Neuron. 54:105–120.
de Vente J, Steinbusch HW, Schipper J. 1987. A new approach to immunocytochemistry of 3′,5′-cyclic guanosine monophosphate: preparation, specificity, and initial application of a new antiserum against formaldehyde-fixed 3′,5′-cyclic guanosine monophosphate. Neuroscience. 22:361–373.
Demyanenko GP, Halberstadt AI, Pryzwansky KB, Werner C, Hofmann F, Maness PF. 2005. Abnormal neocortical development in mice lacking cGMP-dependent protein kinase I. Brain Res Dev Brain Res. 160:1–8.
Dupuy ST, Houser CR. 1996. Prominent expression of two forms of glutamate decarboxylase in the embryonic and early postnatal rat hippocampal formation. J Neurosci. 16:6919–6932.
Dzhala V, Talos D, Sdrulla D, Brumback A, Mathews G, Benke T, Delpire E, Jensen F, Staley K. 2005. NKCC1 transporter facilitates seizures in the developing brain. Nat Med. 11:1205–1213.
Eilers J, Plant T, Marandi N, Konnerth A. 2001. GABA-mediated Ca2+ signalling in developing rat cerebellar Purkinje neurones. J Physiol. 536:429–437.
Garthwaite J. 2008. Concepts of neural nitric oxide-mediated transmission. Eur J Neurosci. 27:2783–2802.
Garthwaite J, Southam E, Boulton C, Nielsen E, Schmidt K, Mayer B. 1995. Potent and selective inhibition of nitric oxide-sensitive guanylyl cyclase by 1H-[1,2,4]oxadiazolo[4,3-a]quinoxalin-1-one. Mol Pharmacol. 48:184–188.
Ge S, Goh E, Sailor K, Kitabatake Y, Ming G, Song H. 2006. GABA regulates synaptic integration of newly generated neurons in the adult brain. Nature. 439:589–593.
Giuili G, Luzi A, Poyard M, Guellaen G. 1994. Expression of mouse brain soluble guanylyl cyclase and NO synthase during ontogeny. Brain Res Dev Brain Res. 81:269–283.
Groneberg D, Koesling D, Friebe A. 2008. Evaluation of ODQ as specific inhibitor of NO-sensitive guanylyl cyclase using mice deficient for the enzyme. Basic Clin Pharmacol Toxicol. 102:40.
Hajos N, Ellender TJ, Zemankovics R, Mann EO, Exley R, Cragg SJ, Freund TF, Paulsen O. 2009. Maintaining network activity in submerged hippocampal slices: importance of oxygen supply. Eur J Neurosci. 29:319–327.
Khazipov R, Esclapez M, Caillard O, Bernard C, Khalilov I, Tyzio R, Hirsch J, Dzhala V, Berger B, Ben-Ari Y. 2001. Early development of neuronal activity in the primate hippocampus in utero. J Neurosci. 21:9770–9781.
Koesling D, Russwurm M, Mergia E, Mullershausen F, Friebe A. 2004. Nitric oxide-sensitive guanylyl cyclase: structure and regulation. Neurochem Int. 45:813–819.
Kullmann PH, Kandler K. 2008. Dendritic Ca2+ responses in neonatal lateral superior olive neurons elicited by glycinergic/GABAergic synapses and action potentials. Neuroscience. 154:338–345.
Makara JK, Katona I, Nyiri G, Nemeth B, Ledent C, Watanabe M, de Vente J, Freund TF, Hajos N. 2007. Involvement of nitric oxide in depolarization-induced suppression of inhibition in hippocampal pyramidal cells during activation of cholinergic receptors. J Neurosci. 27:10211–10222.
McLean HA, Caillard O, Khazipov R, Ben-Ari Y, Gaiarsa JL. 1996. Spontaneous release of GABA activates GABAB receptors and controls network activity in the neonatal rat hippocampus. J Neurophysiol. 76:1036–1046.
Mohajerani MH, Cherubini E. 2006. Role of giant depolarizing potentials in shaping synaptic currents in the developing hippocampus. Crit Rev Neurobiol. 18:13–23.
Morales-Medina J, Mejorada A, Romero-Curiel A, Flores G. 2007. Alterations in dendritic morphology of hippocampal neurons in adult rats after neonatal administration of N-omega-nitro-L-arginine. Synapse. 61:785–789.
Murray AJ, Peace AG, Shewan DA. 2009. cGMP promotes neurite outgrowth and growth cone turning and improves axon regeneration on spinal cord tissue in combination with cAMP. Brain Res. 1294:12–21.
Namiki S, Kakizawa S, Hirose K, Iino M. 2005. NO signalling decodes frequency of neuronal activity and generates synapse-specific plasticity in mouse cerebellum. J Physiol. 566:849–863.
Nikonenko I, Boda B, Steen S, Knott G, Welker E, Muller D. 2008. PSD-95 promotes synaptogenesis and multiinnervated spine formation through nitric oxide signaling. J Cell Biol. 183:1115–1127.
Nikonenko I, Jourdain P, Muller D. 2003. Presynaptic remodeling contributes to activity-dependent synaptogenesis. J Neurosci. 23:8498–8505.
Prast H, Philippu A. 2001. Nitric oxide as modulator of neuronal function. Prog Neurobiol. 64:51–68.
Sánchez-Islas E, León-Olea M. 2004. Nitric oxide synthase inhibition during synaptic maturation decreases synapsin I immunoreactivity in rat brain. Nitric Oxide. 10:141–149.
Sipila ST, Huttu K, Soltesz I, Voipio J, Kaila K. 2005. Depolarizing GABA acts on intrinsically bursting pyramidal neurons to drive giant depolarizing potentials in the immature hippocampus. J Neurosci. 25:5280–5289.
Sipila ST, Schuchmann S, Voipio J, Yamada J, Kaila K. 2006. The cation-chloride cotransporter NKCC1 promotes sharp waves in the neonatal rat hippocampus. J Physiol. 573:765–773.
Szabadits E, Cserep C, Ludanyi A, Katona I, Gracia-Llanes J, Freund TF, Nyiri G. 2007. Hippocampal GABAergic synapses possess the molecular machinery for retrograde nitric oxide signaling. J Neurosci. 27:8101–8111.
Tanaka J, Markerink-van Ittersum M, Steinbusch HW, De Vente J. 1997. Nitric oxide-mediated cGMP synthesis in oligodendrocytes in the developing rat brain. Glia. 19:286–297.
Teunissen C, Steinbusch H, Markerink-van Ittersum M, Koesling D, de Vente J. 2001. Presence of soluble and particulate guanylyl cyclase in the same hippocampal astrocytes. Brain Res. 891:206–212.
Van Staveren WC, Steinbusch HW, Markerink-Van Ittersum M, Repaske DR, Goy MF, Kotera J, Omori K, Beavo JA, De Vente J. 2003. mRNA expression patterns of the cGMP-hydrolyzing phosphodiesterases types 2, 5, and 9 during development of the rat brain. J Comp Neurol. 467:566–580.
Vanhatalo S, Palva JM, Andersson S, Rivera C, Voipio J, Kaila K. 2005. Slow endogenous activity transients and developmental expression of K+-Cl– cotransporter 2 in the immature human cortex. Eur J Neurosci. 22:2799–2804.
Wang D, Kriegstein A. 2008. GABA regulates excitatory synapse formation in the neocortex via NMDA receptor activation. J Neurosci. 28:5547–5558.
Zhang P, Yu P, Tsang A, Chen Y, Fu A, Fu W, Chung K, Ip N. 2010. S-nitrosylation of cyclin-dependent kinase 5 (cdk5) regulates its kinase activity and dendrite growth during neuronal development. J Neurosci. 30:14366–14370.
Zufall F, Shepherd GM, Barnstable CJ. 1997. Cyclic nucleotide gated channels as regulators of CNS development and plasticity. Curr Opin Neurobiol. 7:404–412.